Chemometrics and Intelligent Laboratory Systems 160 (2017) 8–12

Contents lists available at ScienceDirect

Chemometrics and Intelligent Laboratory Systems

journal homepage: www.elsevier.com/locate/chemometrics

Resolution of effects in multi-frequency eddy current data for reliable diagnostics of conductive materials

A.V. Egorov[a], S.V. Kucheryavskiy[b,*], V.V. Polyakov[a,c]

[a] Depatment of Technical Physics, Altai State University, Barnaul, Russia
[b] Department of Chemistry and Bioscience, Aalborg University, Esbjerg, Denmark
[c] Institute of Strength Physics and Materials Science SB RAS, Tomsk, Russia

ARTICLE INFO

Keywords:
Eddy currents
Non-destructive testing
Diagnostics of materials

ABSTRACT

The effect of eddy currents is widely used for diagnostics of conductive materials. It allows to create very simple and inexpensive systems for non-destructive measurements. However, the results of the measurements depend on many factors, including first of all, a conductivity of material and a margin between a sample and a measurement sensor. If both are unknown, it is not possible to evaluate them. The present paper thoroughly reports on an attempt to resolve the influence of the two factors by applying chemometric methods to the eddy current measurements obtained for a set of frequencies.

1. Introduction

Eddy current testing (ECT) is one of the well-known non-destructive methods [1] for inspection of conductive materials including diagnostics, detection of flaws (both on and under surface), cracks, corrosion, evaluation of electrical conductivity, thickness and many other properties [2–5]. The method can be used both with magnetic and non-magnetic objects.

The main part of any ECT device is a sensor, which usually consists of two inductance coils with a magnetic core (or just wire coils in a simple form) [1]. An alternating current (AC) source with preset frequency and amplitude is used to activate one of the coils (usually called a transmitting coil), which creates a changing magnetic field around the sensor. If the sensor is located close to a conductive sample, the magnetic field is being induced to the sample and creates eddy currents, which, in their turn, produce a secondary magnetic field opposed to the primary field generated by the transmitting coil. The second (receiving) coil collects the superposition of the two fields which influence its impedance (reactance and resistance). It is also possible to use a single coil both for inducing the primary field as well as for detecting the superposition of the primary and secondary magnetic fields.

The properties of the secondary field (and, therefore, of the superposition of the two fields) depend on many parameters including type of material (mainly electrical conductivity), its thickness, distance between the sample and the sensor. The properties are also influenced by a presence of any disturbances on or under the sample's surface, such as cracks, scratches, coatings, and other flaws. This actually leads to the one of the biggest disadvantage of the method — its sensitivity depends on many interfering factors and often it is very difficult to resolve them if more than just one are unknown [3].

One of the simplest ways to tackle this problem is to use multi-frequency measurements, when the parameters of the magnetic fields are measured for a range of AC frequencies used to activate the induction coil (activation frequencies) [3,6]. The results of such measurements are often represented in a graphical form using so called scanning hodographs — diagrams showing how resistance and reactance of the receiving coil are changing depending on the activation frequency [7]. This kind of plot is also known as an impedance plane [1]. The shape of the hodographs reflects an influence of the main factors and thorough investigation of the shape as well as comparing the shapes with measurements made for standard objects can be quite useful for analysis and diagnostics [7]. At the same time, such approach is rather subjective, highly dependent on experience of an analyst, and does not allow to carry out automatic measurements. It was also found out that for many real cases (as it will be shown in the present study as well) it is not possible to resolve several influencing factors. Several attempts were made to resolve the influence of the factors for example by using mathematical models based on the Maxwell equations system. However, the results were satisfactory only for a small set of simple and rather artificial cases.

In the present study we propose a use of multivariate approach for resolving the interfering factors in eddy current testing. The general idea is to represent changes in resistance and reactance of the

* Corresponding author.
E-mail address: svk@bio.aau.dk (S.V. Kucheryavskiy).

http://dx.doi.org/10.1016/j.chemolab.2016.11.007
Received 29 September 2016; Received in revised form 31 October 2016; Accepted 16 November 2016
Available online 17 November 2016
0169-7439/ © 2016 Elsevier B.V. All rights reserved.

measuring system obtained at different activating frequencies for a particular sample in a form of a spectrum and use multivariate techniques for finding hidden patterns in the changes, which may mainly reflect an influence of a particular factor.

Despite the simplicity and obviousness of such approach not so many papers devoted to the use of multivariate methods in ETC were found and most of them dealing with more sophisticated technique *pulsed eddy current* (PEC) [8]. Thus in [9] authors used Principal Component Analysis (PCA) for testing its sensitivity for a thickness of a sample and for crack detection. The PCA was applied to differential response signals obtained from a PEC sensor. The results were quite satisfactory, however in this study authors varied only one parameter at time — either a size of a crack or a thickness of a sample. Results of similar analysis but for detection of a defect (a small hole) in aluminum samples has been reported in [10]. We were able to find only one paper [11] were multivariate methods (PCA) were employed for analysis and visualization of traditional multi-frequency eddy-current measurements.

In order to test the feasibility of the proposed approach we investigated a possibility to resolve at least two competing factors, namely a conductivity of a sample and a margin between the sample and a sensor. This paper reports on the main results of the study.

2. Materials and methods

2.1. Eddy current measurements

The measurement system used in the present study included an AC power source, sensor and a simple circuit coupled with data acquisition unit. A computer's sound card was used both for generating the AC signals as well as for reading the changes of voltage and current from the sensor using both channels of analogue input. The system itself and the measurements were controlled using a program written in the LabVIEW environment (National Instruments, Austin, USA). A simplified schematic diagram of the system is shown in Fig. 1.

The power source output signal can be represented in a complex form as follows:

$$\dot{U}_1 = U_1 e^{j\varphi_1}.$$

Here U_1 is an amplitude of the power source signal and φ_1 is its initial phase. The signal goes through the measuring circuit consisted of the sensor with reactance X and resistance R as well as a resistor with resistance r. The resistor converts current in the circuit to a voltage $\dot{U}_2$:

$$\dot{U}_2 = U_2 e^{j\varphi_2}.$$

Here U_2 – is the amplitude and φ_2 – the initial phase of the signal. Then the parameters of the sensor, X and R can be calculated as follows:

$$X = r\frac{U_1}{U_2}sin(\varphi_1 - \varphi_2),$$

$$R = r\left[\frac{U_1}{U_2}cos(\varphi_1 - \varphi_2) - 1\right].$$

The sensor was made as a single coil with a core made from Mg-Ni ferrite magnet with initial relative permeability $\mu = 2000$. The diameter of the sensor was 15 mm.

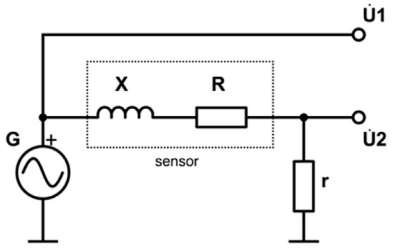

Fig. 1. A schematic diagram of the measurement system.

The measurements were carried out in a frequency range 100–6400 Hz with steps from 50 to 400 Hz (32 frequencies in total). Every measurement resulted in changes of relative resistance computed as $\Delta R/X_0 = (R - R_0)/X_0$ and relative reactance computed as $\Delta X/X_0 = \omega(L - L_0)/X_0$ when a sample is present. Here R and X are parameters of the sensor calculated using (3) and (4); X_0, L_0 and R_0 are resistance, inductivity and reactance of the sensor without a sample; ω is the angular activation frequency. Both parameters were calculated for all activation frequencies resulting in 64 values (ECT signal).

2.2. Samples

The experiments have been planned using full factorial design with five conductivity values and ten values for the margin. The materials included copper ($\sigma = 57 \pm 6$ MS/m), magnesium ($\sigma = 22 \pm 2$ MS/m), bronze ($\sigma = 8.5 \pm 0.8$ MS/m) and two aluminum alloys ($\sigma = 16 \pm 2$ MS/m and $\sigma = 25 \pm 2$ MS/m). The conductivity of the materials was measured using the four-point method with relative uncertainty around 8%.

Five samples of each material were taken for the measurements, each sample looked like a flat plate with thickness about 20 mm. This is much larger than the thickness of a skin-layer for the used frequencies, so the thickness of the samples did not influence the measurements. The ECT signals were measured at different margins between the samples and the sensor. The margins varied from 0 mm to 1 mm and were set by using dielectric films. The margin was measured with a micrometer (uncertainty ± 0.002 mm).

2.3. Representation and analysis of the measured data

The measured relative resistance and reactance were first investigated using traditional approach with hodographs. The points on the plots were colored according to the conductivity and the margin in order to find any association between the shape of the hodographs and values of the two response variables.

On the next step, Principal Component Analysis (PCA) was applied for further exploration of the data. The measured values were mean centered prior to PCA; no other preprocessing has been used. The scores plots were color grouped for the analysis similar to the hodographs.

Finally, Partial Least Squares (PLS) regression was employed for investigation of the associations between ECT measurements, conductivity of the samples and margin used for the measurements. Two separate PLS models were fitted for each of the response variables. The models were validated using repeated random cross-validation with four segments and four repetitions. The model performance was evaluated using graphics with predicted and measured values for response variables as well as coefficient of determination (R^2) and root mean squared error (RMSE) statistics calculated for cross-validated predictions. Variable Importance in Projection (VIP) scores [12] were used for getting knowledge about which frequencies are the most important for predictions.

All calculations and plots were made using R v. 3.3.1 coupled with *mdatools* [13] package.

3. Results and discussion

Fig. 2 shows the measured ECT signals in form of hodographs (top) as well as in form of line plots (bottom). The points and lines are colored according to the conductivity of the samples (left) and margin between the samples and the ECT sensor (right).

In hodographs the points on the top side of the plots correspond to lower frequencies and points on the bottom side to the higher. As one can see, the points corresponding to the samples with different conductivity measured at the same margin are lying on the same curve with a small shift to the bottom (high frequency) part.

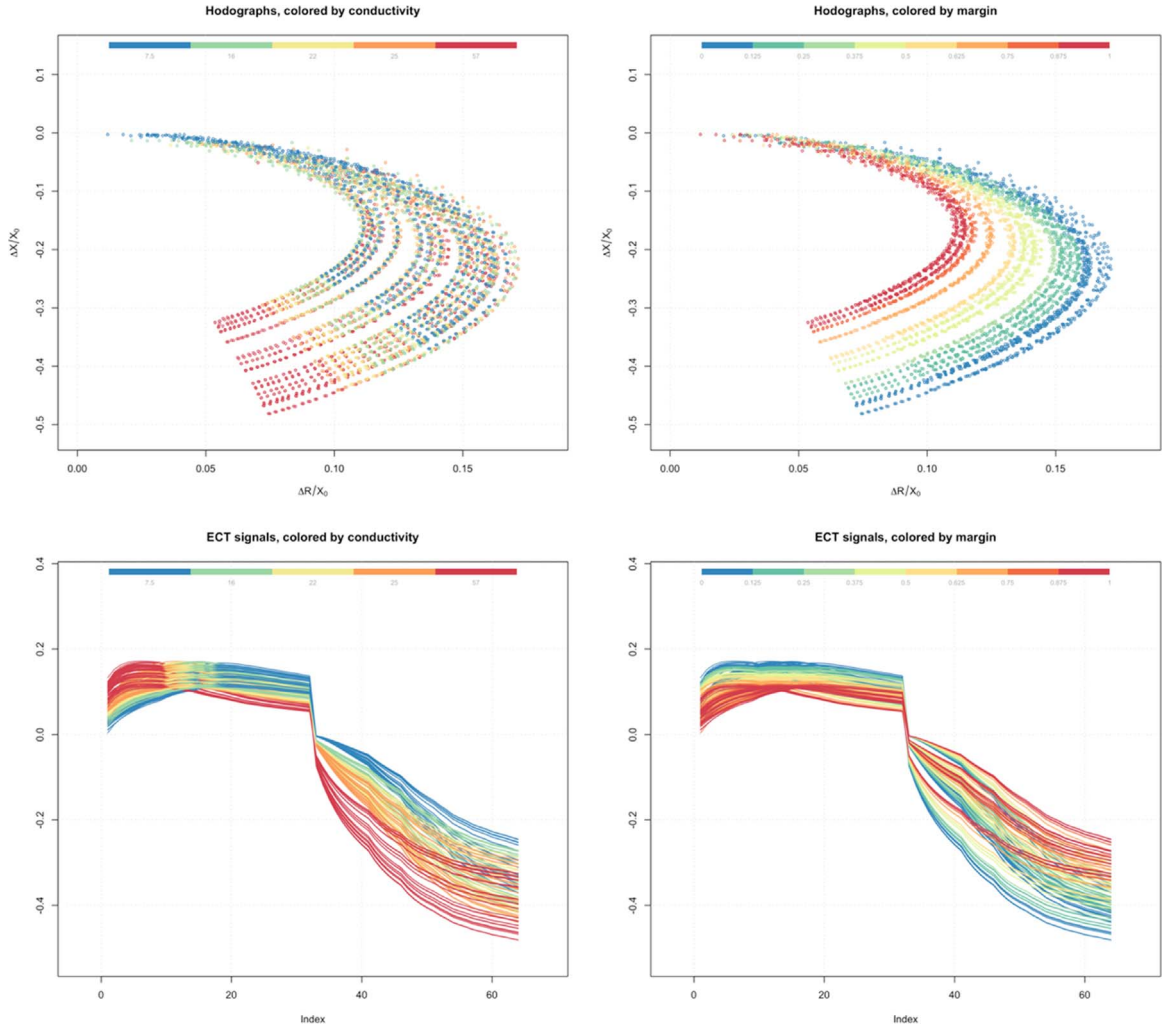

Fig. 2. Representation of measured relative reactance and resistance in form of hodographs (top) and line plots (bottom).

The variation of the margin led to the shift of the points along the x-axis showing a very clear pattern on the hodograph plot, especially for the high frequencies. The main reason for such behavior is that the skin-layer is smaller at high frequencies and, therefore, the margin has a bigger influence on the characteristics of the sensor coil. As one can notice the use of hodographs for representation of the ECT measurements does not allow to resolve the simultaneous influence of conductivity and margin.

The plots in the bottom part of the Fig. 2 are the same measurements but represented in a form of line plots. The left part of each curve

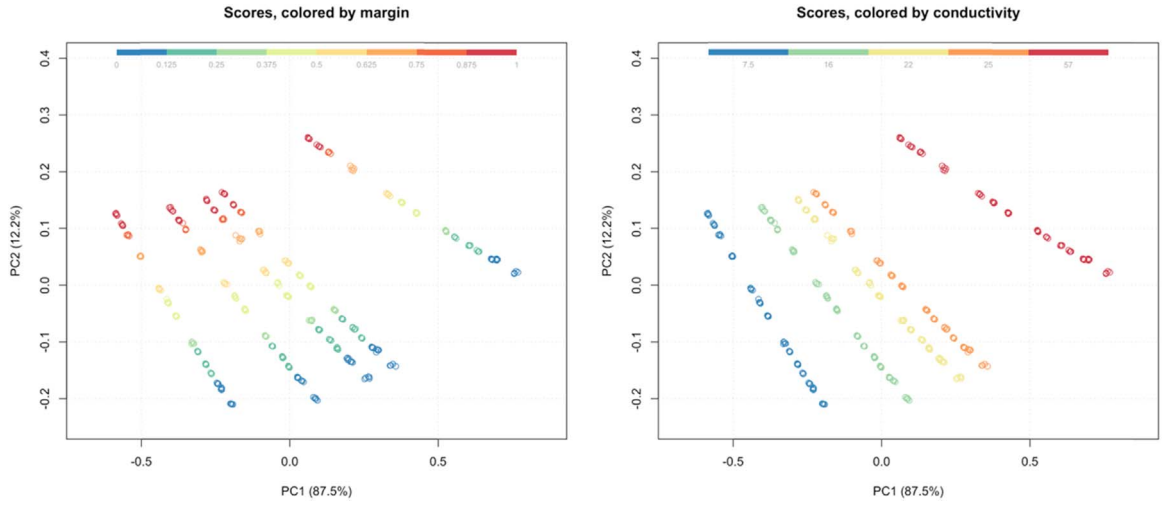

Fig. 3. PCA scores for the first two principal components colored by the margin (left) and conductivity (right) of the samples. (For interpretation of the references to color in this figure legend, the reader is referred to the web version of this article).

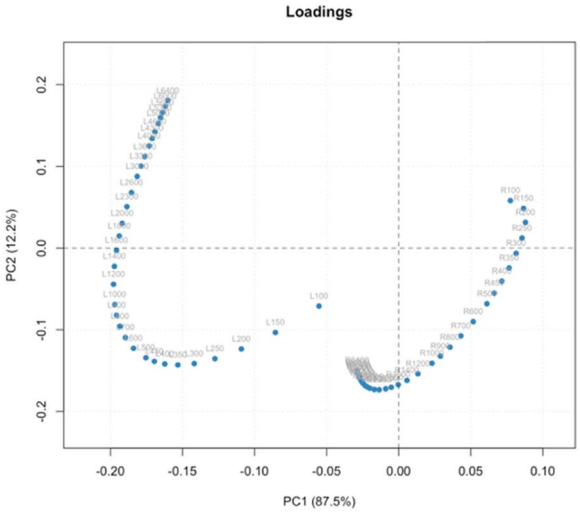

Fig. 4. PCA loadings for the first two principal components.

(first 32 values) shows changes in relative resistance from lower frequencies to higher; and the right part (values from 33 to 64) shows the changes in the reactance. In contrast to the hodographs the line plots show a good separation of the signals obtained for samples with different conductivity (especially for the reactance at low frequencies) but fails to resolve the effect of margin. Also, as it was expected, variation of both parameters influence mostly the reactivity of the system.

Fig. 3 shows scores plots from a PCA model calibrated using the unfolded ECT signals. The points are color grouped according to the conductivity (left) and the margin (right). First two principal component explained almost 99.7% of the data variation and, as one can see from the plots, the scores clearly reflect the changes in both parameters. Distance between group of points on the right plot is proportional to the difference in conductivity of the samples. Analysis of the loadings plot (Fig. 4) also show a clear pattern in the behavior of the variables and variation of the parameters. The point labels denote the type of the variable (*R* for resistance and *L* for reactance) as well as the frequency.

The main results of PLS regression are illustrated in Fig. 5. The top part of the figure shows a VIP scores plot for each model. As one can notice in both cases the resistance values have smaller influence on the predictions. However, as it has been proven experimentally, the use of only reactance values leads to worse models especially in case of margin predictions. Even though the prediction performance statistics did not get significantly worse, the residuals plot showed very clear systematic patterns when resistance is excluded.

The behavior of the reactance values in general meets the expectations and to what have been found from analysis of original signals and the PCA results. High frequencies have a big impact on prediction of margin due to the size of the skin-layer as it was mentioned above.

The reactance measured at low frequencies is more important for prediction of conductivity. This can be explained by the fact that at a

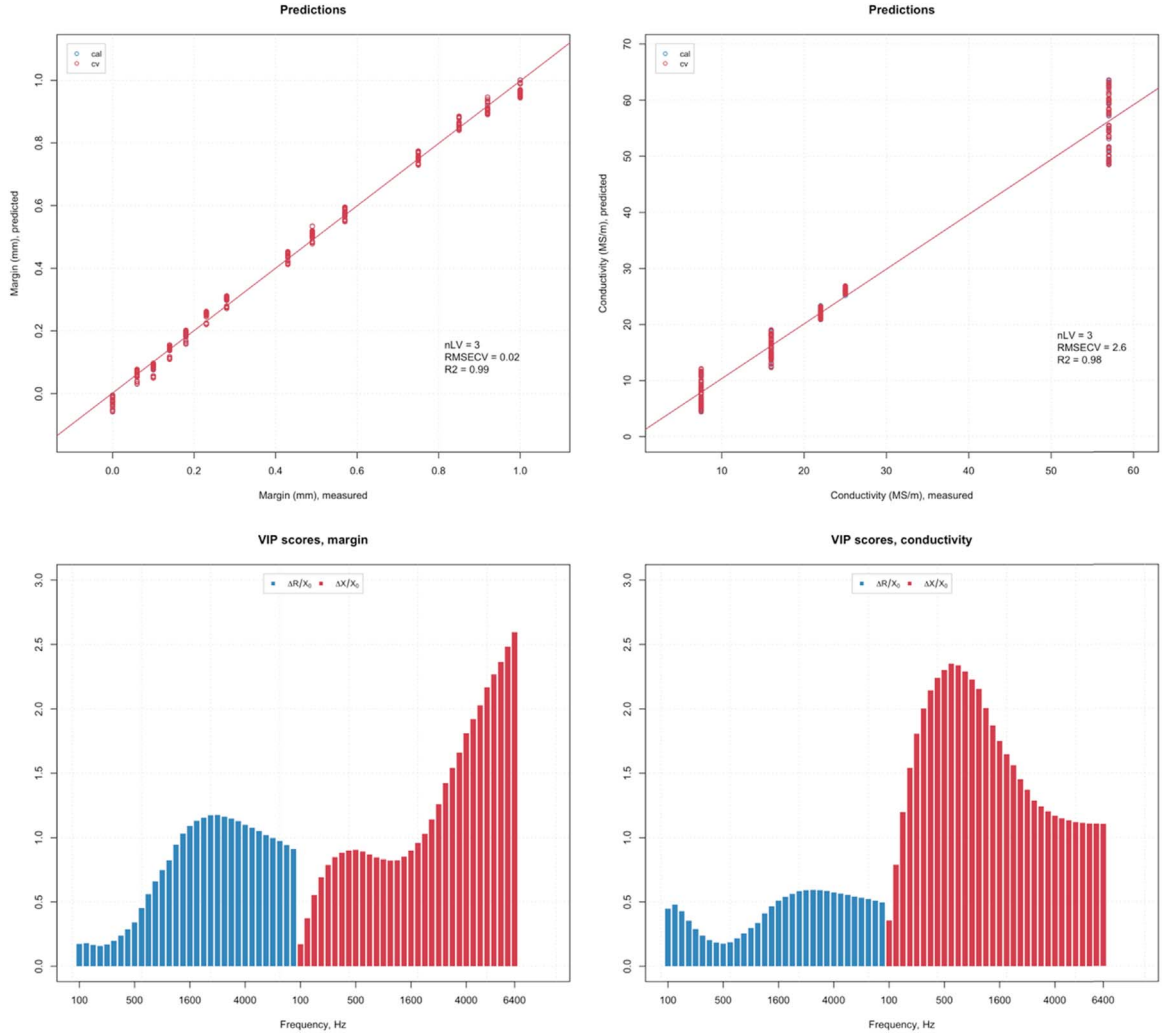

Fig. 5. Predicted vs. measured plots (top) and VIP-scores (bottom) for the PLS regression models.

fixed margin the characteristics of the sensor depend only on the parameter β, which is proportional to a product of sample conductivity and the activation frequency ($\beta \sim \sqrt{\omega\sigma}$). At low frequencies the variation of conductivity dominates and has a main influence to the variation of reactance values. At the same time, the influence of margin to the variation of reactance and resistance at low frequencies is relatively small allowing to resolve the effect from changes in conductivity.

The bottom part of Fig. 5 shows the predicted vs. measured values (with statistics for cross-validated predictions) plot for each of the PLS models. In both cases three latent variables were necessary to achieve a proper prediction quality. The prediction performance for margin was very good (cross-validated $R^2 = 0.99$), however one can notice a small non-linearity pattern in the plot. Indeed, the dependence of the reactivity of a coil on the margin between a sample and a sensor is experimentally proven to be exponential [14]. A non-linear transformation can further improve the model, but, taking into account the excellent performance of the existent model, authors believe this will be unnecessary complication.

Predictions for conductivity looks well for the first four materials and get a bit worse for the copper, which had the highest conductivity value. There are several reasons for such behavior including a possibly small variation of conductivity among individual samples. However, the main reason for such behavior, from our point of view, is that the influence of margin increases for materials with large conductivity as the size of the skin layer gets smaller for good conductors.

4. Conclusions

We have shown that the use of multivariate methods allowed to resolve an influence of competing factors, such as conductivity and margin between a sample and sensor, on the multi-frequency eddy-current measurements. The results are especially good for materials with low and moderate conductivity as in this case the influence of margin is not that larger. This greatly expands the range of applications for eddy-current testing making possible for example measuring of thickness of dielectric coating of metal materials without knowing their composition or conductivity.

This work is a feasibility study and will be the basis for further improving and optimization of the method.

References

[1] J. García-Martín, J. Gómez-Gil, E. Vázquez-Sánchez, Non-destructive techniques based on eddy current testing, Sensors 11 (2011) 2525–2565. http://dx.doi.org/10.3390/s110302525.

[2] Z. Song, T. Yamada, H. Shitara, Y. Takemura, Detection of damage and crack in railhead by using eddy current testing, J. Electromagn. Anal. Appl. 3 (2011) 546–550. http://dx.doi.org/10.4236/jemaa.2011.312082.

[3] A.V. Egorov, V.V. Polyakov, D.S. Salita, E.A. Kolubaev, S.G. Psakhie, A.G. Chernyavskii, et al., Inspection of aluminum alloys by a multi-frequency eddy current method, Defin. Technol. 11 (2015) 99–103. http://dx.doi.org/10.1016/j.dt.2014.12.002.

[4] L.B. Pedersen, M. K.-A, Y. Zhengsheng, Eddy current testing of thin layers using co-planar coils, Res. Nondestruct. Eval. 12 (2000) 53–64.

[5] D. Mercier, J. Lesage, X. Decoopman, D. Chicot, Eddy currents and hardness testing for evaluation of steel decarburizing, NDT E Int. 39 (2006) 652–660. http://dx.doi.org/10.1016/j.ndteint.2006.04.005.

[6] Z. Liu, K. Tsukada, K. Hanasaki, M. Kurisu, Two-dimensional eddy current signal enhancement via multifrequency data fusion, Res. Nondestruct. Eval. 11 (1999) 165–177. http://dx.doi.org/10.1007/PL00003919.

[7] V.G. Atavin, A.I. Terekhov, R.R. Iskhuzhin, V.V. Kuranov, Plotting and analysis of hodographs for studying the electrophysical parameters of objects using attachable eddy-current transducers, Russ. J. Nondestruct. Test. 49 (2013) 595–601. http://dx.doi.org/10.1134/S1061830913100045.

[8] Dongfeng He, M. Yoshizawa, Saw-wave excitation eddy-current nde based on hts rf squid, IEEE Trans. Appl. Supercond. 13 (2003) 3803–3806. http://dx.doi.org/10.1109/TASC.2003.816202.

[9] A. Sophian, G.Y. Tian, D. Taylor, J. Rudlin, A feature extraction technique based on principal component analysis for pulsed Eddy current NDT, NDT E Int. 36 (2003) 37–41. http://dx.doi.org/10.1016/S0963-8695(02)00069-5.

[10] Y. BinFeng, L. FeiLu, H. Dan, Research on edge identification of a defect using pulsed eddy current based on principal component analysis, NDT E Int. 40 (2007) 294–299. http://dx.doi.org/10.1016/j.ndteint.2006.12.005.

[11] S. Shokralla, J.E. Morelli, T.W. Krause, Principal components analysis of multi-frequency eddy current data used to measure pressure tube to calandria tube gap, IEEE Sens. J. 16 (2016) 3147–3154. http://dx.doi.org/10.1109/JSEN.2016.2529721.

[12] I.G. Chong, C.H. Jun, Performance of some variable selection methods when multicollinearity is present, Chemom. Intell. Lab. Syst. 78 (2005) 103–112. http://dx.doi.org/10.1016/j.chemolab.2004.12.011.

[13] S. Kucheryavskiy, R Package for Multivariate Data Analysis, 2016, doi:https://dx.doi.org/10.5281/zenodo.59547.

[14] Y. Yating, D. Pingan, X. Lichuan, Coil impedance calculation of an eddy current sensor by the finite element method, Russ. J. Nondestruct. Test. 44 (2008) 296–302. http://dx.doi.org/10.1134/S1061830908040104.